# Monolithically 3D-Printed Pressure Sensors for Application in Electronic Skin and Healthcare Monitoring

Jinsu Yoon[1†], Bongsik Choi[1†], Yongwoo Lee[1], Jungmin Han[1], Jieun Lee[1], Jinhee Park[1], Yeamin Kim[1], Dong Myong Kim[1], Dae Hwan Kim[1], Min-Ho Kang[2], Sungho Kim[3*], and Sung-Jin Choi[1*]
[1]School of Electrical Engineering, Kookmin University, Seoul, Korea, *Email: sjchoiee@kookmin.ac.kr
[2]Department of Nano-process, National Nanofab Center (NNFC), Daejeon, Korea,
[3]Department of Electrical Engineering, Sejong University, Seoul, Korea, *Email: sungho85kim@sejong.ac.kr
[†]These authors are equally contributed to this work.

***Abstract*****—**The monolithically 3D-printed pressure sensor was demonstrated with excellent sensing performance in terms of sensitivities and reliabilities. The porous-structured dielectric was formed by casting an elastomer prepolymer into 3D-printed water-soluble templates, where the porosities were accurately controlled; hence, the sensing performances can be tuned. The flexible top and bottom electrodes were also monolithically integrated using the 3D-printed conductive thermoplastic. Finally, we presented that our sensors can be applied to the electronic skin with spatial mapping abilities and a wearable healthcare monitoring system.

## I. Introduction

Wearable and flexible pressure sensors have attracted a considerable amount of interest and increasing demands over the last decades in relation to various advanced applications such as electronic skin and textiles, soft robotics, and mobile healthcare aids [1-2]. Various types of pressure sensors including resistive and capacitive sensors have, therefore, been intensively investigated. For capacitive-type pressure sensors, superb advantages have been reported, such as high sensitivity, low power consumption, simple design, and fast response to stimuli [3]. To ensure the implementation of high-performance capacitive pressure sensors, various approaches using microstructured elastomeric dielectric layers [4] and porous elastomeric dielectric layers [5] have been attempted. In particular, the porous elastomeric dielectric layer has outstanding mechanical characteristics such as excellent flexibility, softness, resiliency, and no barreling phenomena, which is required for high-performance pressure sensors [5]. Despite these capabilities, the capacitive-type pressure sensor with a porous-structured dielectric layer has hitherto been largely overlooked because of the limits of manufacturing methods.

In this work, we present a facile and cost-effective approach to fabricate highly sensitive capacitive pressure sensor based on the porous structure of a polydimethylsiloxane (PDMS) thin-film dielectric layer, which is produced using a three-dimensional (3D) printer (Fig. 1). The morphology (specifically, the porosity) of the porous-structured PDMS layer in our capacitive-type pressure sensor can be accurately controlled by adjusting the densities of the water-soluble, 3D-printed polyvinyl alcohol (PVA) templates with no complicated fabrication processes. Therefore, the sensing performances, which include sensitivity, of the pressure sensor can be easily tuned by using the 3D printer. Moreover, using a 3D printer, the bendable and flexible top and bottom electrodes of the pressure sensor were monolithically printed from the conductive thermoplastic (conductive polylactic acid, CPLA) with no additional processes. Hence, a facile, cost-effective fabrication of high-performance pressure sensors is feasible. Our fabricated 3D-printed flexible pressure sensors can detect extremely low pressures and enable real-time tactile sensing applications with a wide dynamic range of pressures. The porous-structured pressure sensor with 80% porosity exhibited high sensitivity up to 0.591 $kPa^{-1}$, high stability over more than 1200 cycles of applied pressure, and a short response time. Finally, this sensor was pixelated into a flexible 3 × 3 array, which indicates that such sensors can be applied in real-time tactile spatial mapping systems for electronic skin applications. Moreover, our 3D-printed pressure sensor was applied to a wearable healthcare monitoring system. Therefore, our 3D-printed pressure sensor may open a new gateway for applications in advanced human-machine interface systems.

## II. Fabrication And Characterization

Fig. 2 show the schematic illustration of our monolithically 3D-printed pressure sensor and its fabrication processes. First, the CPLA layer was printed as a bottom electrode through the heated nozzle in the 3D printer at 240 ℃. Then, the water-soluble PVA layer was printed through the heated nozzle at 190 ℃ to form the template of the porous PDMS layer in the pressure sensor. During the 3D printing, the PVA densities of 40% to 80% were accurately controlled. Then, a top CPLA electrode was printed under the identical conditions as the bottom electrode. Next, the 3D-printed structure was fully covered with the PDMS prepolymer solution and heated at 80 ℃ for 3 hours. By casting the PDMS prepolymer in the 3D-printed PVA template and dissolving the PVA template, the porous-structured PDMS was created (Fig. 3). The porosities of the porous-structured PDMS layer can accurately be controlled by adjusting the PVA densities during the 3D printing based on the need of individual applications, which was confirmed from the microscope images of the sensors with various porosities

(Fig. 4). Our monolithically 3D-printed pressure sensor has high flexibility and bendability (Fig. 5). Detailed information of the 3D-printed pressure sensor is shown in Table I.

## III. Results and Discussion

When the porosities in the PDMS layer were increased, the initial capacitance values of the 3D-printed pressure sensors gradually decreased because the dielectric constant of air ($\varepsilon_{Air} = 1$) was smaller than the dielectric constant of PDMS ($\varepsilon_{PDMS} \approx 3$) (Fig. 6). We also confirmed that the measured values were similar to the predicted values through the formula for calculating the effective dielectric constant. The 3D-printed pressure sensor performance was examined by plotting the curves of the external pressure input (P) vs. the relative change in capacitance ($\Delta C/C_0$, where $C_0$ is the initial capacitance) for the sensors with the porous-structured PDMS and solid PDMS layers. The curves were obtained using custom-designed equipment for applying and detecting various pressure levels (Fig. 7). The sensitivity (S) is defined as the slope of the curves, i.e., $S = \delta(\Delta C/C_0) / \delta P$. Note that, the sensitivities of our pressure sensors clearly increased with the porosities in the porous-structured PDMS layer (Fig. 8). The clear enhancement in sensitivity of the pressure sensors with increasing porosity is attributed to the decreasing stiffness. Thus, a much larger capacitance change can be obtained with an identical pressure input. Furthermore, the capacitance change can be boosted by the increase in effective dielectric constant with gradual closure of the pores under external pressure.

Fig. 9 shows the capacitive responses of the 3D-printed pressure sensors with various porosities for the identical external pressure (11.11 kPa). The capacitive responses of the porous-structured pressure sensors were obviously enhanced with the increasing porosity. Fig. 10 also shows that our sensors produce an excellent match between the pressure input profiles and the response curves with continuous, stable, noise-free, and perfectly reversible signals through dynamic testing at various pressures. In addition, the reliability of our pressure sensor was evaluated by applying 1200 or more repeated compression/release cycles (in the pressure range of 0-1.1 kPa) to the sensor with 80% porosity to investigate its long-term stability and mechanical durability (Fig. 11). No drift of the sensor responses and no structural changes of the 3D-printed pressure sensor with the porous-structured PDMS were found during 1200 compression/release cycles.

In addition, we evaluated the hysteresis in the sweep range of 0-33.3 kPa with various sweep rates (Figs. 12 and 13). The hysteresis of the pressure sensor with 0% porosity (i.e., the solid PDMS layer) increased at higher sweep rates, whereas the hysteresis of the 3D-printed pressure sensor with 80% porosity was completely negligible at all sweep rates. Because the pores can reduce the viscoelastic property of the PDMS, such remarkable reversible sensor responses can be achieved without noticeable hysteresis. We summarized the hysteresis of the sensors with the porous-structured PDMS and solid PDMS layers in Fig. 14.

For a deeper investigation of the applicability of our 3D-printed pressure sensor to wearable pressure-sensing devices, our sensor was used in a bandage-type pressure-sensing device to detect human wrist pulse signals (Fig. 15). As a control group, we also compared the sensor signal on the palm, where there is no skin deflection induced by the bloodstream. As shown in Fig. 16, the sensor signal on the wrist was clearly identified (84 beats/min) compared to the noise level from the sensor attached on the palm. Furthermore, general clinical information such as the arterial stiffness, which is related to the age of people, could also be collected and identified from the zoom-in view of the sensor signals from the wrist (Fig. 17). Two distinguishable peaks ($P_1$ and $P_2$ at $t_1$ and $t_2$, respectively) were obtained, which could be used to estimate clinical information. The radial artery augmentation index ($P_2$ / $P_1$) and time distance ($t_2 - t_1$) were measured to be 0.461 and 449 ms, respectively. The results were consistent with the reference data, which are comparable with the values expected for a healthy adult male in his late twenties [6].

Finally, a pressure sensor array was monolithically fabricated using a 3D printer to detect spatially distributed pressures in a 2D space. A flexible 3D-printed pressure sensor array with $3 \times 3$ pixels was designed (Fig. 18a) and fabricated (Fig. 18b). Then, stamps patterned with arithmetic operation "1 + 6 = 7" were applied to the sensor array (Fig. 18c, top). Each number and symbol was successfully recognized by the proposed 3D-printed pressure sensor array (Fig. 18c, bottom). As mentioned, the porous PDMS layer does not produce any significant barreling phenomena, so the effect of neighboring sensor cells is negligible.

## IV. Conclusion

We demonstrated the monolithically 3D-printed flexible pressure sensor with a porous-structured PDMS layer. The porosity in the porous PDMS layer was accurately controlled by adjusting the densities of the water-soluble 3D-printed PVA templates, and the flexible electrodes using the conductive thermoplastic, such as CPLA, in the pressure sensor were monolithically integrated with no additional processes. Excellent sensing performances were obtained ($S = 0.591\ kPa^{-1}$). In addition, the sensors had outstanding reliability and stability over 1200 compressing/releasing cycles. To investigate its applicability to wearable devices, a bandage-type wrist-pulse-monitoring device and a spatially applied pressure detecting device array were demonstrated.

## Acknowledgment

This work was supported by the National Research Foundation (NRF) of Korea under Grants 2016R1A2B4011366 and 2016R1A5A1012966 and partially by the Future Semiconductor Device Technology Development Program (Grant 10067739) funded by MOTIE (Ministry of Trade, Industry & Energy) and KSRC (Korea Semiconductor Research Consortium).

## References

[1] W. Gao, *et al.*, *Nature*, **529**, 509, 2016.
[2] T. Someya, *et al.*, *Proc. Natl. Acad. Sci. U. S. A.*,**101**, 9966, 2004.
[3] S. Kang, *et al.*, *Adv. Electron. Mater.*, **2**, 1600356, 2016.
[4] S. C. B. Mannsfeld, *et al.*, *Nat. Mater.*, **9**, 859, 2010.
[5] D. Kwon, *et al.*, *ACS Appl. Mater. Interfaces*, **8**, 16922, 2016.
[6] S. C. Millasseau, *et al.*, *Clin. Sci.*, **103**, 371, 2002

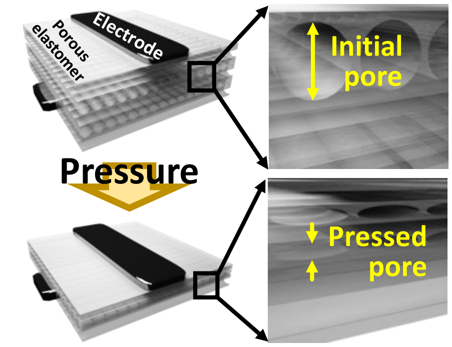


**Fig. 1** Device structure of the monolithically 3D-printed capacitive-type pressure sensor with the porous-structured dielectric before and after an external pressure was applied.

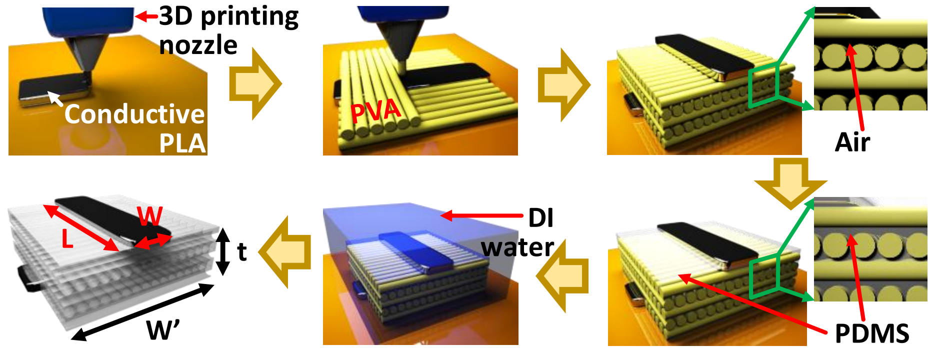


**Fig. 2** Fabrication processing steps of the monolithically 3D-printed pressure sensor with the porous PDMS layer. The flexible conductive thermoplastic (conductive polylactic acid, CPLA) was printed as the top and bottom electrodes of the pressure sensor. A polyvinyl alcohol (PVA) template was printed to form the porous PDMS layer.

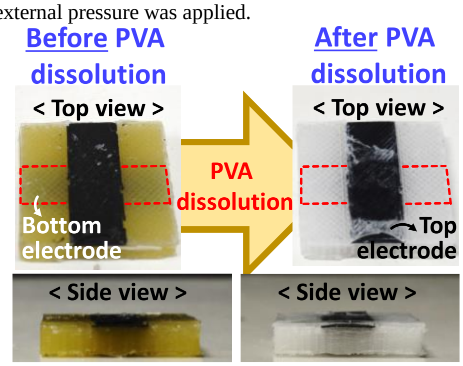


**Fig. 3** Photographs of the 3D-printed pressure sensors before and after the dissolution of the 3D-printed PVA template.

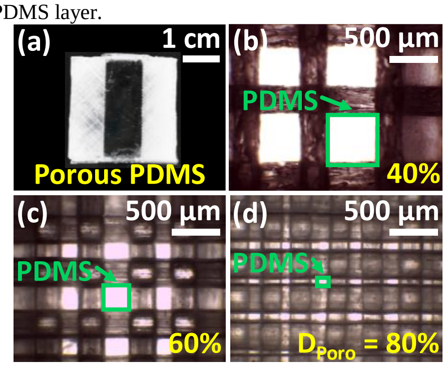


**Fig. 4** (a) 3D-printed pressure sensor after the dissolution of PVA; (b)-(d) microscope images of the porous PDMS with various porosities ($D_{Poro}$) (40-80%).

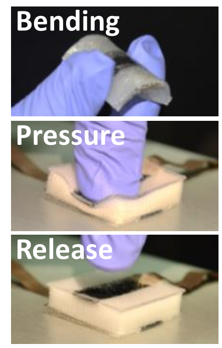


| Parameter | Value |
|---|---|
| Nozzle diameter | 0.4 mm |
| Length (L) | 3 mm |
| Width (W) | 10 mm |
| Thickness (t) | 3 mm |
| PVA one layer thickness | 0.3 mm |
| Total width (W') | 30 mm |

**Fig. 5** Photographs of the flexibility, softness, and resiliency of the 3D-printed pressure sensor with porous-structured PDMS. (Table I. Key parameters for the 3D-printed pressure sensor)

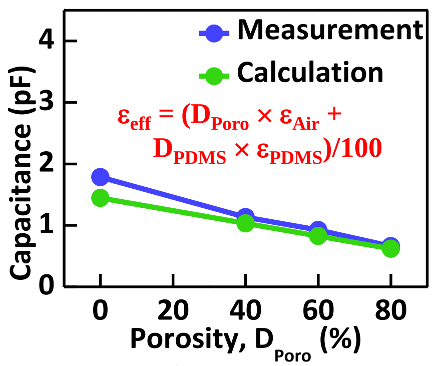


**Fig. 6** Comparison of the measured and calculated capacitance values of the 3D-printed pressure sensor with various porosities. $D_{Poro}$ and $D_{PDMS}$ in $\varepsilon_{eff}$ refer the volume proportions of the air and PDMS.

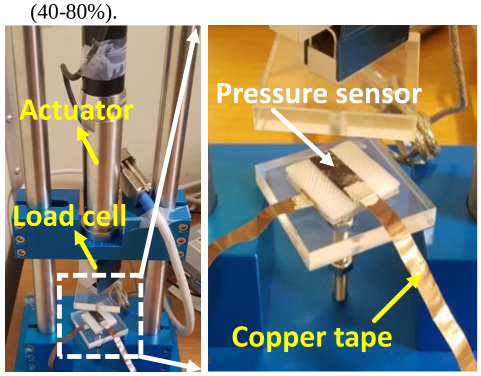


**Fig. 7** Pressure testing machine and measurement method. The copper tape was used to connect with the LCR meter to measure the capacitance changes.

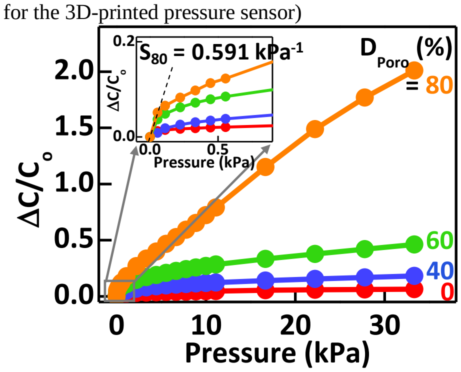


**Fig. 8** Relative change in capacitance of the 3D-printed pressure sensors with four different porosities in the PDMS (0, 40, 60, and 80%).

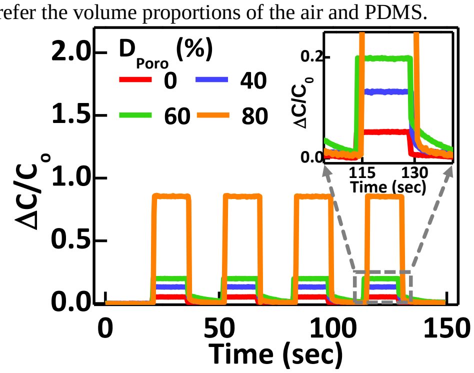


**Fig. 9** Dynamic responses of the 3D-printed pressure sensors with different porosities of 0, 40, 60, and 80% under the same pressure of 11.11 kPa.

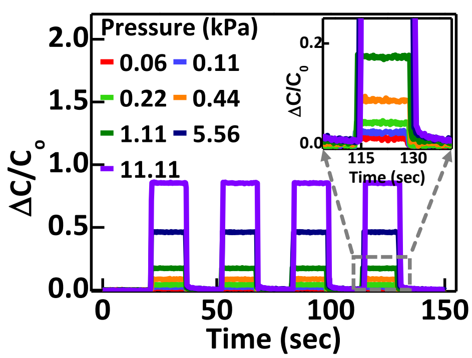


**Fig. 10** Dynamic responses of the 3D-printed pressure sensors with 80% porosity under various pressure levels.

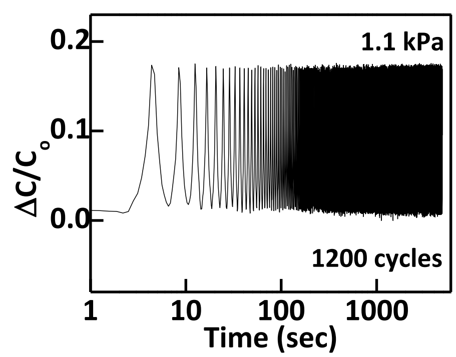


**Fig. 11** Pressure sensor reliability test (1200 cycles). In each cycle, the pressure was swept from 0 to 1.1 kPa.

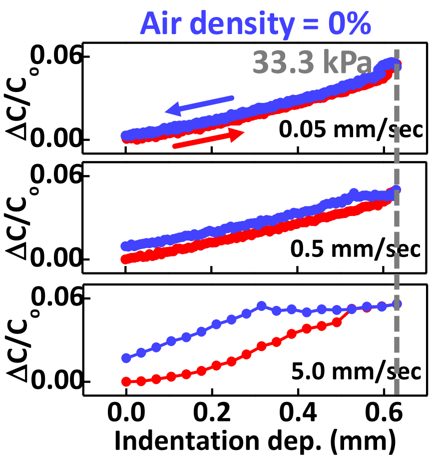


**Fig. 12** Hysteresis characteristics of the 3D-printed pressure sensor with 0% porosity in response to different sweep rates (0.05, 0.5, and 5.0 mm/sec). The red line was measured at a forward sweep. The blue line was measured at a reverse sweep.

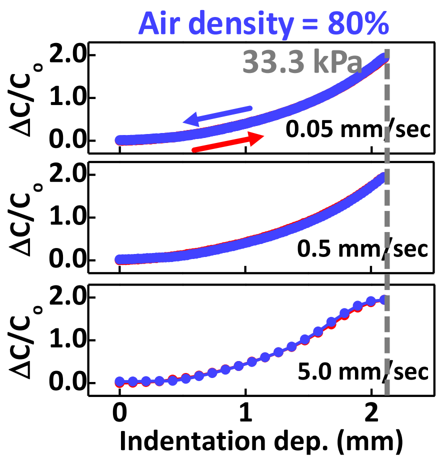


**Fig. 13** Hysteresis characteristics of the 3D-printed pressure sensor with 80% porosity in response to different sweep rates (0.05, 0.5, and 5.0 mm/sec). The red line was measured at a forward sweep. The blue line was measured at a reverse sweep.

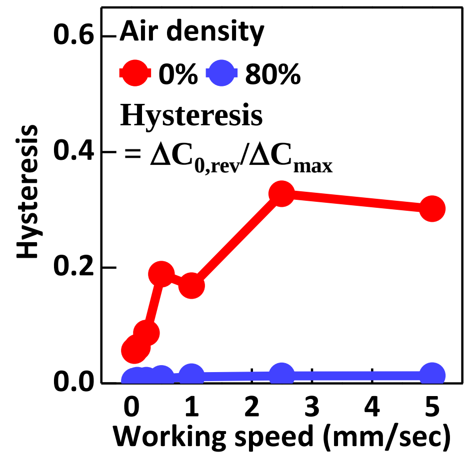


**Fig. 14** Comparison of the hysteresis performance in the sensors with the porous-structured PDMS and solid PDMS layers. $\Delta C_{0,rev}$ and $\Delta C_{max}$ in the equation refer to the difference in capacitance of forward and reverse sweep at 0 kPa and the maximum change of capacitance, respectively.

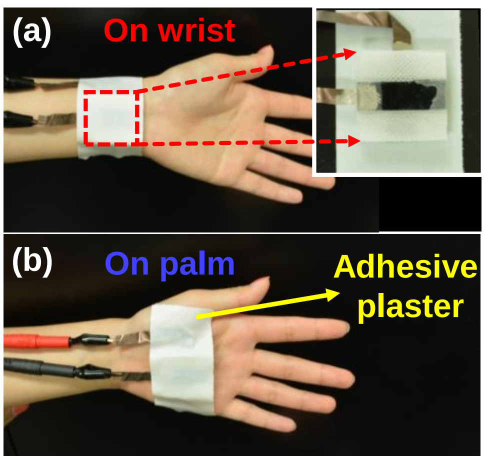


**Fig. 15** Mounting of the 3D-printed pressure sensor onto a human wrist (a) and palm (b) with commercial adhesive plaster.

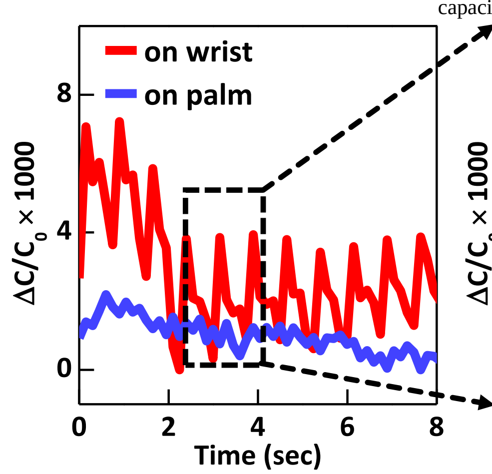


**Fig. 16** Relative change in capacitance of the 3D-printed pressure sensor with 80% porosity on the wrist and palm. The red line was measured on the wrist. The blue line was measured on the palm.

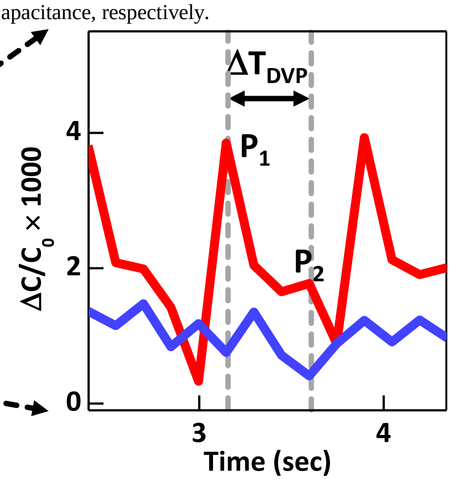


**Fig. 17** Zoom-in view of the obtained signal, which shows two peaks $P_1$ and $P_2$ at $t_1$ and $t_2$, respectively.

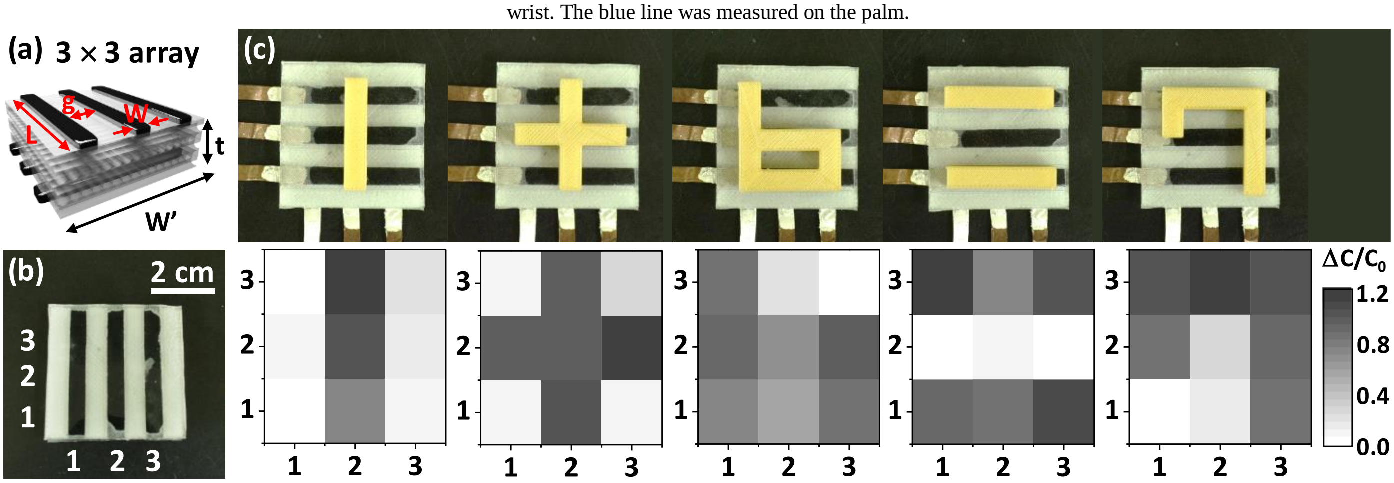


**Fig. 18** Application of the 3D-printed pressure sensor array (3 × 3) with the porous-structured PDMS dielectric layer to electronic skin to detect the spatial pressure distributions in a two-dimensional space. (a) Schematic image of the pressure sensor array with 3 × 3 pixels. (b) Photograph of the 3D-printed 3 × 3 pressure sensor array (L = 39 mm; W = 5 mm; W' = 39 mm; t = 3 mm; porosity = 80%; distance between adjacent electrodes g = 6 mm). (c) Photographs of the measurement setups to detect the spatially distributed pressure in a 2D space (top) and recognize the pressure distribution on the pressure sensor array by applying stamps patterned with the numbers and symbols "1", "+", "6", "=", and "7".